ACS APPLIED MATERIALS & INTERFACES

Research Article

Cite This: ACS Appl. Mater. Interfaces 2019, 11, 17306−17312

www.acsami.org

Robust Serum Albumin-Responsive AIEgen Enables Latent Bloodstain Visualization in High Resolution and Reliability for Crime Scene Investigation

Zhaoyu Wang,[†] Pengfei Zhang,[†] Haixiang Liu,[†] Zheng Zhao,[†,‡] Linghong Xiong,[⊥] Wei He,[†] Ryan T. K. Kwok,[†,‡] Jacky W. Y. Lam,[†,‡] Ruquan Ye,*[,§] and Ben Zhong Tang*[,†,‡,∥]

[†]Department of Chemistry, Hong Kong Branch of Chinese National Engineering Research Center for Tissue Restoration and Reconstruction, Institute of Advanced Study, Division of Life Science and State Key Laboratory of Molecular Neuroscience. The Hong Kong University of Science and Technology, Kowloon 999077, Hong Kong, China

[‡]HKUST-Shenzhen Research Institute, Shenzhen 518057 China

[§]Department of Chemistry, City University of Hong Kong, Kowloon 99077, Hong Kong, China

[∥]Guangdong Innovative Research Team, SCUT-HKUST Joint Research Laboratory, State Key Laboratory of Luminescent Materials and Devices, South China University of Technology, Guangzhou 510640 China

[⊥]Shenzhen Center for Disease Control and Prevention, Shenzhen 518055, China

Supporting Information

ABSTRACT: Bloodstains provide admissible information for crime scene investigators. The ability to resolve latent bloodstains that are commonly found in real scenarios is therefore pivotal to public security. Here, we report a facile approach for invisible bloodstain visualization based on the click reaction between serum albumin and tetraphenylethene maleimide (TPE-MI), an aggregation-induced emission luminogen (AIEgen). Compared to the widely adopted methods based on the harsh catalytic oxidation activity of hemoglobin, this working principle benefits from the specificity of the mild catalyst-free thiol−ene click reaction that improves the reliability and resolution. In addition, the mild conditions preserve DNA information and bloodstain patterns, and the excellent photophysical properties of the AIEgen afford high sensitivity and stability (>1 yr). Such an excellent performance cannot be achieved by conventional AIEgens and aggregation-caused quenching luminogens with similar structures. TPE-MI outperforms the benchmark luminol-based technique in visualizing latent bloodstains as showcased in two mock crime scenes: spattered blood track and transfer blood fingerprint. This disclosed method is an advancement in forensic science that could inspire future development of technology for bloodstain visualization.

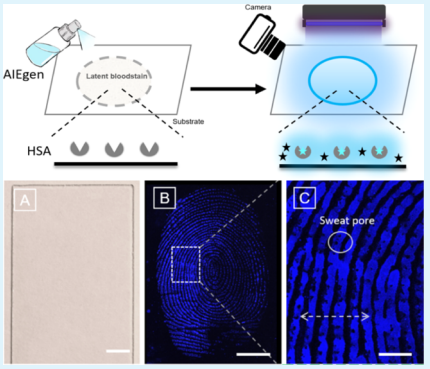

KEYWORDS: *forensic science, aggregation-induced emission, bloodstain detection, thiol probe, public security*

INTRODUCTION

Public security is not only one of the most fundamental human needs but also a prerequisite to economic stability and growth. The advancement of forensic science has drastically improved public safety.[1] Forensic technologies have successfully aided the law enforcement through the provision of admissible evidence for the identification of perpetrators and protection of victims, increasing the cost and risks of committing a crime, possibly preventing future crimes.[2] According to statistics published by the FBI, 1 247 321 violent crimes were committed in the United States in 2017,[3] which averages to 3400 violent crimes per day. In many cases, blood is involved in the violent crime scenes, which provides solid evidence for crime scene investigation and reconstruction.[4,5] However, to escape punishment, perpetrators may clean crime scenes to remove and eliminate possible evidence. Even if the scene is intact and undamaged, it can still be challenging to directly collect a bloodstain pattern in real scenarios. Therefore, the development of forensic technology to retrieve latent bloodstains and differentiate bloodstain patterns from potential background interference is necessary for crime scene investigators (CSI) to collect evidence.[6]

In pursuit of higher resolution, sensitivity, and reliability for bloodstain visualization, various techniques have been hitherto demonstrated. Early strategies based on the color change of dye molecules such as phenolphthalein (Kastle−Meyer), 3,3′,5,5′-tetramethylbenzidine (TMB), and leucomalachite green (LMG) were plagued by their low sensitivity and poor contrast.[7] Because of the capability to provide high sensitivity, methodologies based on fluorescence have now been widely

Received: March 14, 2019
Accepted: April 25, 2019
Published: April 25, 2019

DOI: 10.1021/acsami.9b04269
ACS Appl. Mater. Interfaces 2019, 11, 17306−17312

Scheme 1. Mechanism and Equipment Setup of Blood Detection with TPE-MI[a]

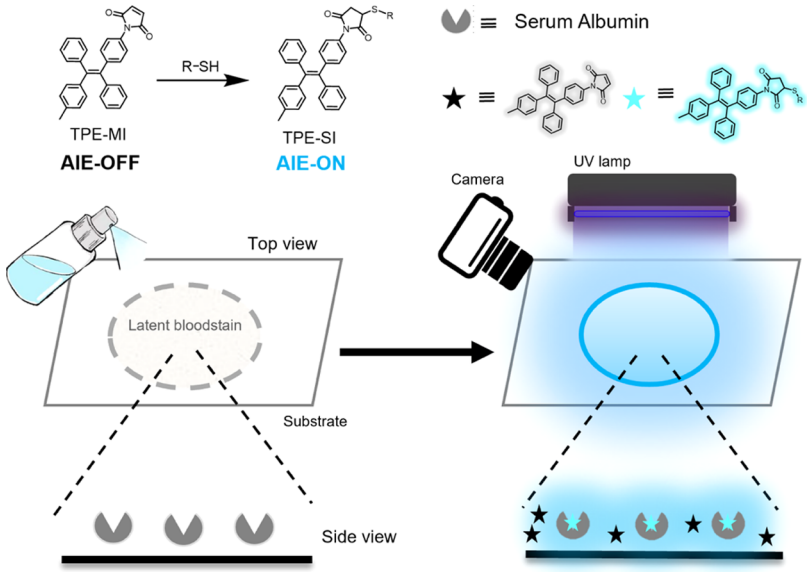

[a]The surface with latent bloodstain is sprayed by TPE-MI solution and the bloodstain becomes blue-emissive under UV irradiation.

adopted as the main pathway for bloodstain visualization. This forensic technique is commonly established from the catalytic oxidation activity of hemoglobin in blood, which can be represented by the commercially available fluorescein-based[8] and luminol-based[9] products. The working mechanism of fluorescein-based products is based on photoluminescence (PL), whereas that of luminol is based on chemiluminescence (CL). Although their use in bloodstain visualization has been successfully demonstrated by CSI in certain investigations, there are many drawbacks in both systems. First, fluorescein is hampered by photobleaching[10] and the duration of luminol CL is extremely short, which impedes the collection of admissible evidence. Second, both systems require the use of fresh samples prepared from laborious protocols. For example, fluorescein-based methods involve a nasty activation step using zinc powder, and luminol requires the storage under low temperature and away from light because of its instability.[11] Third, false positive fluorescence could arise in the presence of other catalysts from the background, including but not limited to metal ions (rust, soil, bacterial, or plant pigments) and oxidants (bleach, horseradish sauce, and some fruits).[12] Fourth, both systems involve a harsh condition that could be destructive and interfere with the collection of other information. For instance, zinc powder used in the fluorescein-based product will destroy the DNA, and H_2O_2 employed in the luminol product is oxidative.[13] Therefore, the development of a new nondestructive approach for bloodstain detection to address the aforementioned weaknesses is highly desirable.

Herein, we report a new strategy for bloodstain visualization based on the mild catalyst-free thiol−ene click reaction between human serum albumin (HSA) and tetraphenylethene maleimide (TPE-MI) dye[14] (Scheme 1). We chose HSA as the target because it is the most abundant protein in blood (~43 g/L) and it constitutes ~60% of total plasma protein.[15] In addition, the free thiol group of HSA can function as a turn-on reactant and the protein cavity will restrict the intramolecular motion of the fluorophore, which will enhance the TPE fluorescence. This phenomenon was described by the aggregation-induced emission (AIE) effect, which suggests that the restriction of intramolecular motion (RIM) will favor the radiative decay of the dye and improve its fluorescence.[16−18] Compared to other AIE luminogens (AIEgens) that fluoresce strongly in the solid/aggregate state, TPE-MI is nonemissive in the aggregation state until the conjugation between the carbonyl and olefin groups of MI is disrupted through an addition reaction with a thiol group forming an emissive product, namely, tetraphenylethene succinimide (TPE-SI) (Scheme 1).[19] The strong emission of TPE-SI combined with structural advantages of HSA enables the development of a high-sensitivity and high-contrast forensic technique. In addition, the specificity of the turn-on mechanism improves the reliability, and the nondestructive nature of the method allows the acquisition of additional important information such as transfer fingerprint that cannot be achieved using the conventional approaches.

EXPERIMENTAL SECTION

Preparation and Development of Bloodstains. Original blood was collected from a healthy white rabbit, fed and kept in Animal & Plant Care Facility, HKUST. Blood (5 mL) was collected from the rabbit every time with heparin to cause little effect on the health of the rabbit. Human blood was collected from a healthy donator from Shenzhen Center for Disease Control and Prevention. All the experiments were conducted following the rules of HKUST ethics committee. All blood experiments were done with rabbit blood, except that the mock crime scene spattered bloodstain (Figure 4) was prepared with human blood.

Blood diluted with phosphate-buffered saline (1×) by a factor of 10, 100, and 1000 was dropped (5 μL) on a glass slide or other substrates. Then, it was dried for 1 day at room temperature to form a bloodstain. Several drops of TPE-MI solution or luminol/H_2O_2 working solution were dripped on the bloodstain to cover the bloodstain area. The developed bloodstain was documented by photography under UV irradiation or in dark.

Blood Fingerprint Development. A thumb was dipped with diluted blood (dilution factor: 100) first and then pressed on the glass slide. The slide with latent blood fingerprint was soaked in the TPE-MI (250 μM) solution for 5 min. The extra solution drops on the slide were blown by compressed air. The photo was taken under 365

DOI: 10.1021/acsami.9b04269
ACS Appl. Mater. Interfaces 2019, 11, 17306−17312

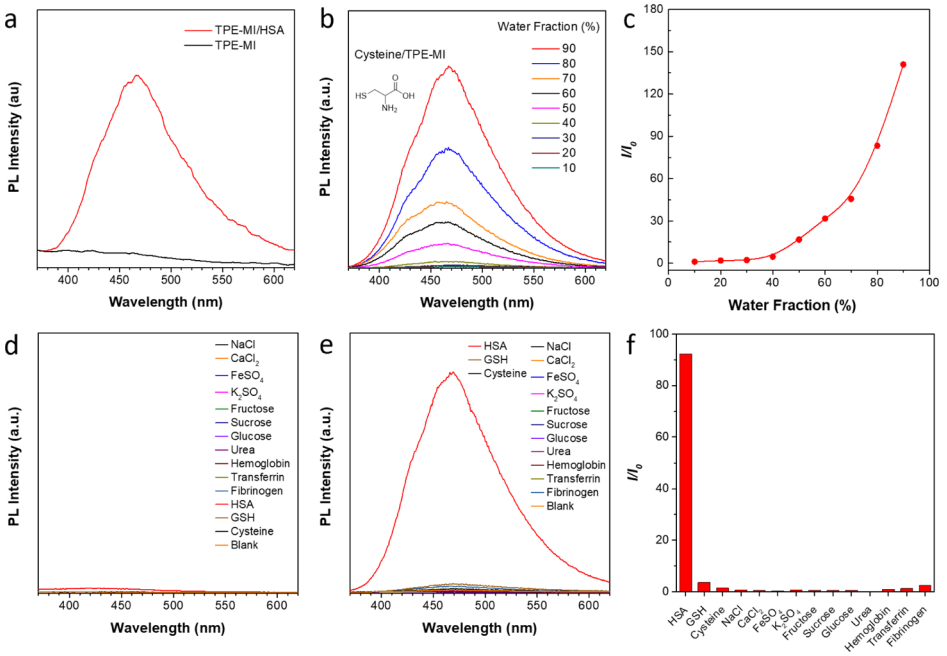

Figure 1. (a) PL spectra of TPE-MI/HSA (10 μM) and pure TPE-MI (10 μM) in the 90% water fraction solvent. (b) PL spectra of TPE-MI (10 μM) and cysteine (100 μM) in DMSO/water mixtures with various water fractions. (c) Plot of relative PL intensity (I/I_0) at 470 nm vs the water fraction composition of the DMSO/water mixtures of TPE-MI/cysteine. (d,e) PL spectra of HSA (3 mg/mL), GSH, cysteine, sodium chloride, calcium chloride, iron(II) sulfate, potassium sulfate, fructose, sucrose, glucose, urea (100 μM), and some proteins in plasma including hemoglobin (0.01 mg/mL), transferrin (0.25 mg/mL), and fibrinogen (0.2 mg/mL) (d) before and (e) after addition of TPE-MI (250 μM) in the (d) 100% and (e) 10% water fraction solvent, respectively. (f) Bar graph of PL emission of TPE-MI with different targets at 470 nm. Excitation: 335 nm.

nm and it was also scanned by a confocal microscope. Meanwhile, another latent blood fingerprint was sprayed by luminol (1.3 mM) working solution. The photo was taken immediately after the spraying of luminol working solution, as the CL vanishes quickly especially for diluted blood.

RESULTS AND DISCUSSION

Photophysical Properties. To validate the method, we first studied the PL properties by recording a series of PL spectra in dimethyl sulfoxide (DMSO)/water mixtures. Pure TPE-MI under aggregation state (90% water fraction) shows negligible emission (Figure 1a, black line). Upon reaction with HSA and cysteine, a strong peak at 470 nm was observed at different fractions of DMSO/water mixture as shown in Figure 1a,b, respectively. Cysteine/TPE-MI presented a typical AIE feature, whose emission became stronger with the increase of water fraction owing to the aggregation of fluorophore in high water content (Figure 1c). There are 35 cysteines in HSA, of which 34 form disulfide bonds and only one is free.[20] By comparing with the PL spectrum of cystine/TPE-MI as shown in Figure S1, it can be concluded that TPE-MI specifically reacts with thiol group rather than disulfide group.

We further evaluated the viability of other components in blood to trigger the emission. The PL of diverse salts (sodium chloride, calcium chloride, iron(II) sulfate, potassium sulfate), small molecules [glutathione (GSH), cysteine, fructose, sucrose, glucose, urea], and proteins (hemoglobin, transferrin, fibrinogen) was measured in a concentration analogous to that in blood in the absence (Figure 1d) and presence (Figure 1e) of TPE-MI, and the on-off intensity ratios (I/I_0) are summarized in Figure 1f. A 10% water fraction solvent is used as it is analogous to the bloodstain visualization protocol, which uses a DMSO solution of TPE-MI so that the interference from thiol-containing small molecules can be mitigated. As expected, HSA plays a key role in activating the emission of TPE-MI compared with other components. Even for small molecules containing a thiol group such as GSH[21] and cysteine, the fluorescence enhancement was not significant for lack of RIM induced by the protein cavity. Such specificity of fluorescent mechanism reduces the chance of interference from environment and improves the reliability of blood detection.

Bloodstain Detection Performance. The turn-on mechanism of TPE-MI demonstrates its potential use in bloodstain visualization. Here, we further evaluate its effectiveness as compared to luminol, the most common method adopted by CSI because of its higher sensitivity compared with other approaches.[7] Blood diluted by a factor from 1 to 1000 was dropped on glass slides and dried in air, resulting in bloodstains ranging from visible to latent (Figure 2a–d). A solution of TPE-MI or luminol working solution was then applied to the bloodstains and photos were taken. However, because luminol is unstable and its working solution expires in less than 1 day, the luminol powder has to be protected from light and high temperature and its solution should be freshly prepared. For TPE-MI, it can be stored in ambient conditions and its solution has a shelf life of over 6 months, which makes the process more convenient and practical.

In comparison with the bloodstains visualized by luminol, TPE-MI exhibits extraordinary sensitivity (Figure 2). Clearly, TPE-MI is capable of specifically detecting the blood area when illuminated with both 254 and 365 nm UV lamps (Figures 2e–h and S3). Even though the bloodstain was hardly recognizable by naked eye at a dilution factor of 1000, the cyan emission of TPE-MI can still be captured to identify the area of blood and visualize its pattern in high resolution and high

DOI: 10.1021/acsami.9b04269
ACS Appl. Mater. Interfaces 2019, 11, 17306–17312

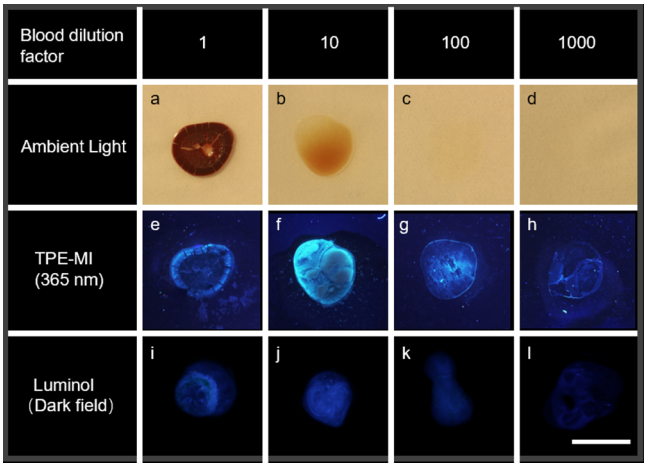

Figure 2. Bloodstain development with TPE-MI and luminol on a glass slide. (a–d) Bloodstain photographs taken under ambient light. (e–h) Fluorescence photographs of bloodstains developed with TPE-MI (2.5 mM) taken under 365 nm UV excitation. (i–l) Photographs of bloodstains developed with (0.4 mM) luminol/H_2O_2 working solution taken in dark. Scale bar: 1 cm.

contrast. On the contrary, although luminol can indicate the presence of bloodstains from CL, the blurry emission especially for diluted blood provides insufficient resolution to describe the features of the bloodstain (Figure 2i–l). Even worse, false signals could sometimes be generated as shown in Figure S5, which might result from the diffusion of oxidation catalysts.

Another advantage of using TPE-MI is its longevity in projecting the bloodstain. The use of luminol can be plagued by the inherently fast oxidation process. Figure 3a shows the CL spectra recorded within 5 min and the peak intensity is summarized in Figure 3b. The CL intensity decayed exponentially and became negligible in 250 s. In comparison, the PL intensity of TPE-MI decreased by less than 30% after continuous strong laser illumination for 35 min (Figure 3b), demonstrating its excellent photostability. The advantage of using TPE-MI is more prominent when the collection of admissible information is needed. As shown in Figure 3c–f, no significant decrease in fluorescence intensity was observed within 30 days. Even for bloodstains that had been developed with TPE-MI and kept in open air after 1 year, the fluorescence remained strong to clearly delineate the bloodstain pattern (Figure 3g–h). However, the bloodstain feature unraveled by luminol fades rapidly and becomes barely detectable by naked eye after 42 s (Figure 3i). Such a short time window could be troublesome for CSI to recognize and photograph bloodstains especially when visualizing a large area.

In addition to the higher sensitivity and stability of TPE-MI than that of luminol, its advantage in bloodstain visualization was further demonstrated in comparison to other dyes. For example, another AIEgen, sodium 1,2-bis[4-(3-sulfonatopropoxyl)phenyl]-1,2-diphenylethene (BSPOTPE), was reported for the visualization of HSA conformation during unfolding process in solution.[22] However, it fails to resolve the bloodstain as BSPOTPE is emissive at solid state even without the presence of blood (Figure S6). For a dye with an aggregation-caused quenching[23] feature such as fluorescein-5-maleimide, it is also inappropriate for bloodstain visualization as its solution is emissive and the emission is independent of the blood (Figure S7). The viability of TPE-MI in forensic

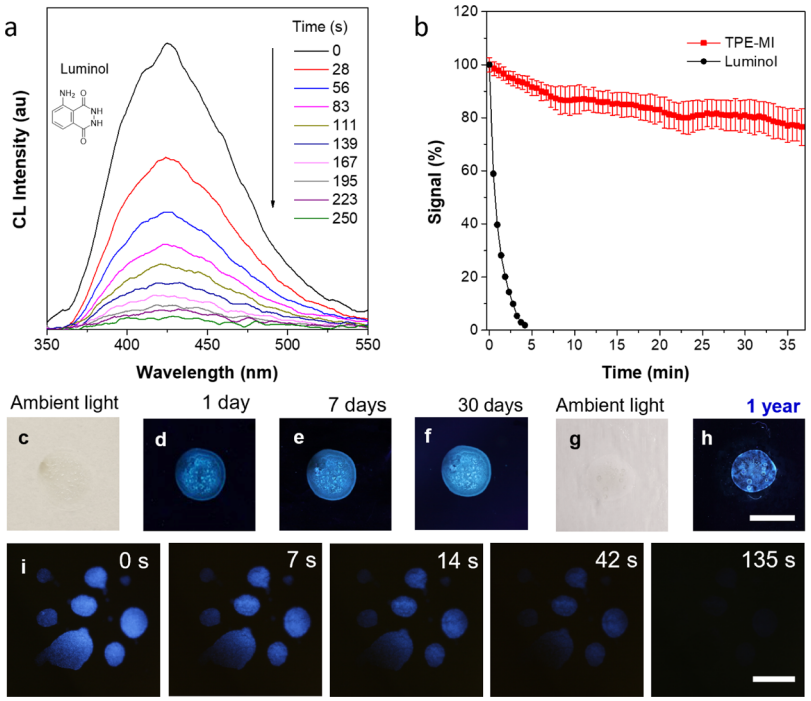

Figure 3. (a) Kinetic CL spectra of luminol/H_2O_2 working solution in diluted blood. [Luminol] = 400 μM, blood dilution factor = 100 ×. (b) Comparison of fluorescence signals. Black line: signal intensity (%) of luminol over time; red line: photostability of TPE-MI (2.5 mM) excited with a 405 nm laser at a power of 0.10 mW. Data were taken at an increment of 11.1 s for 37 min. (c–h) Bloodstain visualized with TPE-MI on the glass slide. (c,g) Typical latent bloodstains stained with TPE-MI in ambient light within 1 month and after 1 year, respectively. (d–f,h) Stained bloodstains aged for 1, 7, 30 d, and 1 y under 365 nm UV light, respectively. (i) Photos of bloodstains sprayed with 1.3 mM luminol/H_2O_2 working solution. Scale bar: 1 cm in (c–h); 5 cm in (i).

DOI: 10.1021/acsami.9b04269
ACS Appl. Mater. Interfaces 2019, 11, 17306–17312

applications is further demonstrated by the ability to unravel the aging bloodstain patterns on universal surfaces. For instance, for bloodstains that have been exposed to open air for 25 days, the treatment with TPE-MI can still successfully retrieve the pattern (Figure S8). For a bloodstain on various surfaces, including nonporous surfaces such as glass, metal, and plastics and porous surfaces such as cotton and cellulose paper, the shape of the bloodstain remains distinguishable from the backgrounds even in the presence of autofluorescent interference (Figures S9 and 4).

Application in Crime Scene Investigation. We finally demonstrate the advantage of using TPE-MI for the extrapolation of critical information from bloodstains in crime scenes. The first important information is the track of latent bloodstains for crime scene reconstruction. Figure 4a shows a mock crime scene by first spattering blood on a 20 × 20 cm glass slide and then rinsing with water until the original pattern becomes invisible by the naked eyes. The glass slide was further aged for 14 days to mimic the real scenario of a homicide. Then, the surface was sprayed with TPE-MI solution (Figure 4b). Under UV illumination, the latent bloodstain pattern was fully retrieved in comparison to the pristine bloodstain (Figure 4a,c). Figure 4d,e shows the same enlarged area of the pristine bloodstain and the TPE-MI-treated latent bloodstain. Clearly, both the track of blood and the spattered pattern was successfully recovered in high resolution. Such information will not only indicate the involvement of blood in crime but also be informative for CSI as it may aid in distinguishing a homicide from a suicide by analyzing the bloodstain pattern.

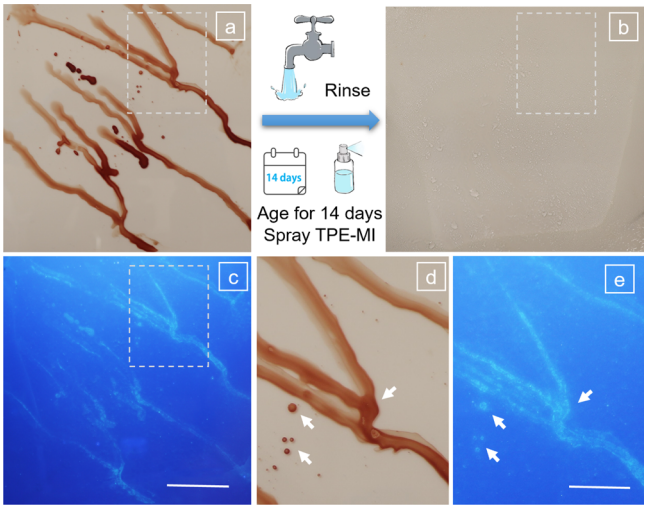

Figure 4. Demonstration of bloodstain visualization in mock crime scenes: retrieval of washed bloodstain patterns (a) pristine blood splattered on a glass substrate (back side of a 20 cm × 20 cm silica gel thin-layer chromatography glass plate). The blood was then rinsed with water and aged for 14 d. Then, the glass surface was sprayed with TPE-MI (2.5 mM) and photos were taken under (b) ambient light and (c) 365 nm UV lamp. (d,e) Enlarged areas indicated in (a,c), respectively. Scale bar: 5 cm in (a–c); 2 cm in (d,e).

A more significant application of TPE-MI is its ability to visualize transfer bloodstains in crime scenes for the direct identification of criminals. Transfer bloodstains play a significant role in crime scene investigation because they result from existing blood in contact with criminal, leaving patterns behind such as shoeprints and fingerprints.[24] The retrieval of fingerprints is extremely useful as it provides direct evidence of whether a suspect was involved in the crime. Figure 5a shows a latent fingerprint prepared from a thumb dipped with diluted blood. Upon treatment of TPE-MI, the fingerprint can be visualized in high resolution. As shown in Figure 5b, the global whorl pattern of ridge flow, the Level 1 fingerprint feature, can be easily distinguished. Further analysis of the local pattern of minutiae, the Level 2 fingerprint feature as shown in the enlarged area in Figure 5c, discloses the characteristic bifurcation, crossover, and ending feature[25] of the fingerprint. More strikingly, the Level 3 feature, which refers to the fine structure of pores on the ridges,[26] can be clearly reflected as circled in Figure 5c. These types of information provide implicit evidence for the identification of suspects that is rarely reported.[27,28] We further compare with the fingerprint feature developed from the luminol working solution. Unfortunately, the fingerprint is fragmentary and unclear (Figure 5d). Because of the generation of vast bubbles from H_2O_2, a majority of the fingerprint pattern was destroyed (Figure 5e). Even for a limited area where certain fingerprint features emerged (Figure 5f), the resolution is poor and whether the minutiae and pore structures originated from the bubbles or the characteristic of fingerprint was inconclusive. In

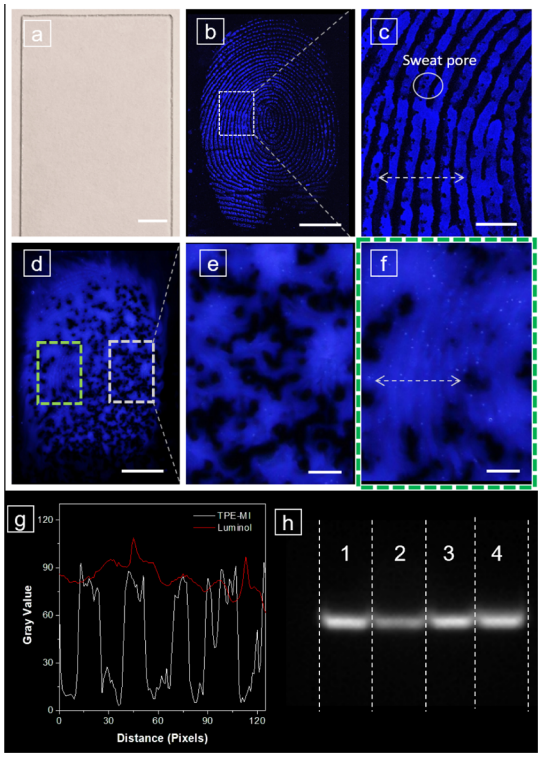

Figure 5. Retrieval of latent blood fingerprint in mock crime scene. Photos of a latent blood fingerprint on a glass slide developed with TPE-MI taken (a) under ambient light, and (b) by a confocal microscope under 405 nm irradiation. (c) Enlarged area in (b) to show the Level 2 and Level 3 fingerprint features. (d) Photo of transfer fingerprint treated with luminol working solution taken in dark field. (e,f) Enlarged white and green dashed squared areas of (d), respectively. Scale bar: 5 mm in (a,b,d); 1 mm in (c,e,f). (g) Gray value analysis of the dashed lines in (c,f). (h) Agarose gel electrophoresis of single-stranded DNA. Lane 1: no treatment (control); lane 2: treated with luminol (1 mM); lane 3: treated with TPE-MI (200 μM); and lane 4: treated with TPE-MI (500 μM).

DOI: 10.1021/acsami.9b04269
ACS Appl. Mater. Interfaces 2019, 11, 17306−17312

comparison to the signal-to-noise ratio (Figure 5g) of the fingerprint feature[29] as indicated by the dashed lines in Figure 5c,f, the method using TPE-MI outperformed that of luminol.

In addition to the useful information from the blood track and transfer pattern, the nondestructive nature of TPE-MI to DNA further validates its applicability in forensic science because DNA samples are collected after the location of the bloodstain. As shown in Figure 5h, the gel electrophoresis result showed that even at high concentrations, TPE-MI did not degrade DNA and interfere with subsequent DNA analyses, which is similar to that of luminol. However, other approaches based on fluorescein-based formulas such as TMB and LMG will interfere with the DNA analysis.[9]

CONCLUSIONS

In conclusion, we have developed a facile method for the presumptive test of blood based on the mild thiol−ene click reaction between HSA and TPE-MI in mild conditions. Taking advantage of the chemical and photophysical properties of TPE-MI, latent bloodstains can be resolved in high resolution and high contrast over a long period (>1 yr). In addition, the specificity of the turn-on mechanism not only improves the reliability but also allows the collection of additional evidence such as latent blood track and fingerprint pattern that cannot be accomplished using prevailing approaches based on the catalytic oxidization of hemoglobin. Other merits such as simple-processing, applicability to fresh and aging bloodstain on universal substrates, and nondestructive nature to DNA further validate its practical use for bloodstain visualization. In cases when other biofluid such as semen coexists with blood, it might interfere with the bloodstain pattern analysis and the application of luminol-based method could strengthen the reliability of bloodstain detection. Yet because TPE-MI is nondestructive to DNA, locating a biofluid or blood using TPE-MI is an important presumptive test for the collection of admissive DNA information. This study is an important advancement in forensic science and could inspire future development of fluorescent approaches for bloodstain visualization.

ASSOCIATED CONTENT

Supporting Information

The Supporting Information is available free of charge on the ACS Publications website at DOI: 10.1021/acsami.9b04269.

Detailed experimental procedure (PDF)

AUTHOR INFORMATION

Corresponding Authors

*E-mail: ruquanye@cityu.edu.hk (R.Y.).
*E-mail: tangbenz@ust.hk (B.Z.T.).

ORCID

Zhaoyu Wang: 0000-0002-8453-643X
Haixiang Liu: 0000-0002-0894-1812
Ryan T. K. Kwok: 0000-0002-6866-3877
Ruquan Ye: 0000-0002-2543-9090
Ben Zhong Tang: 0000-0002-0293-964X

Notes

The authors declare the following competing financial interest(s): A provisional patent using TPE-MI for bloodstain visualization has been filed.

ACKNOWLEDGMENTS

The authors are grateful for the financial support from the National Science Foundation of China (21788102 and 81871523), the Research Grants Council of Hong Kong (16308016, 16305015, N-HKUST604/14, and C2014-15G, C6009-17G), the Innovation and Technology Commission (ITC-CNERC14SC01, ITCPD/17-9, and ITS/254/17), and the Science and Technology Plan of Shenzhen (JCYJ20160229205601482 and JCYJ20160428150429072), Program for Young Innovative Research Team in China University of Political Science and Law (18CXTD09 and 16CXTD05). R.Y. acknowledges the support from Start-Up Grant of the City University of Hong Kong (7200600). Z.W. would like to thank Xinhui Zou for her assistance on drawing the scheme.

REFERENCES

(1) Ortmeier, P. J. *Public Safety and Security*; Gulf Professional Publishing, 2007.
(2) Petherick, W.; Turvey, B.; Ferguson, C. *Forensic Criminology*; Academic Press, 2014.
(3) 2017 Crime in the United States. ucr.fbi.gov/crime-in-the-u.s/2017/crime-in-the-u.s.-2017/topic-pages/violent-crime (accessed on March 2019).
(4) Dutelle, A. *An Introduction to Crime Scene Investigation*; Jones & Bartlett Publishers, 2011.
(5) Bevel, T.; Gardner, R. M. *Bloodstain Pattern Analysis with an Introduction to Crime Scene Reconstruction*; CRC Press, 2008.
(6) Reno, J.; Marcus, D.; Robinson, L.; Brennan, N.; Travis, J. *Crime Scene Investigation: A Guide for Law Enforcement*; U.S. Department of Justice, 2000.
(7) Webb, J. L.; Creamer, J. I.; Quickenden, T. I. A Comparison of the Presumptive Luminol Test for Blood with Four Non-Chemiluminescent Forensic Techniques. *Luminescence* **2006**, *21*, 214−220.
(8) Cheeseman, R. Fluorescein Bloodstain Detection Method. U.S. Patent 5,976,886 A, 1999.
(9) Blackledge, R. D. *Forensic Analysis on the Cutting Edge*; Wiley-Interscience, 2007.
(10) Song, L.; Hennink, E. J.; Young, I. T.; Tanke, H. J. Photobleaching Kinetics of Fluorescein in Quantitative Fluorescence Microscopy. *Biophys. J.* **1995**, *68*, 2588−2600.
(11) Barni, F.; Lewis, S. W.; Berti, A.; Miskelly, G. M.; Lago, G. Forensic Application of the Luminol Reaction as a Presumptive Test for Latent Blood Detection. *Talanta* **2007**, *72*, 896−913.
(12) Quickenden, T. I.; Creamer, J. I. A Study of Common Interferences with the Forensic Luminol Test for Blood. *Luminescence* **2001**, *16*, 295−298.
(13) Frisch, A. M.; Jefferson, C.; Hernández, B. M.; Miguel, I. The Use of Polilights in the Detection of Seminal Fluid, Saliva, and Bloodstains and Comparison with Conventional Chemical-Based Screening Tests. *J. Forensic Sci.* **2006**, *51*, 109−116.
(14) Liu, Y.; Yu, Y.; Lam, J. W. Y.; Hong, Y.; Faisal, M.; Yuan, W. Z.; Tang, B. Z. Simple Biosensor with High Selectivity and Sensitivity: Thiol-Specific Biomolecular Probing and Intracellular Imaging by AIE Fluorogen on a TLC Plate through a Thiol-Ene Click Mechanism. *Chem.—Eur. J.* **2010**, *16*, 8433−8438.
(15) Turell, L.; Carballal, S.; Botti, H.; Radi, R.; Alvarez, B. Oxidation of the Albumin Thiol to Sulfenic Acid and Its Implications in the Intravascular Compartment. *Braz. J. Med. Biol. Res.* **2009**, *42*, 305−311.
(16) Mei, J.; Leung, N. L. C.; Kwok, R. T. K.; Lam, J. W. Y.; Tang, B. Z. Aggregation-Induced Emission: Together We Shine, United We Soar! *Chem. Rev.* **2015**, *115*, 11718−11940.
(17) Zhu, C.; Kwok, R. T. K.; Lam, J. W. Y.; Tang, B. Z. Aggregation-Induced Emission: A Trailblazing Journey to the Field of Biomedicine. *ACS Appl. Bio Mater.* **2018**, *1*, 1768−1786.

DOI: 10.1021/acsami.9b04269
ACS Appl. Mater. Interfaces 2019, 11, 17306−17312

(18) Chong, K. C.; Hu, F.; Liu, B. AIEgen Bioconjugates for Specific Detection of Disease-Related Protein Biomarkers. *Mater. Chem. Front.* **2019**, *3*, 12−24.
(19) Girouard, S.; Houle, M.-H.; Grandbois, A.; Keillor, J. W.; Michnick, S. W. Synthesis and Characterization of Dimaleimide Fluorogens Designed for Specific Labeling of Proteins. *J. Am. Chem. Soc.* **2005**, *127*, 559−566.
(20) Fanali, G.; di Masi, A.; Trezza, V.; Marino, M.; Fasano, M. Human serum albumin: From bench to bedside. *Mol. Aspects Med.* **2012**, *33*, 209−290.
(21) Richie, J. P.; Skowronski, L.; Abraham, P.; Leutzinger, Y. Blood Glutathione Concentrations in a Large-Scale Human Study. *Clin. Chem.* **1996**, *42*, 64−70.
(22) Hong, Y.; Feng, C.; Yu, Y.; Liu, J.; Lam, J. W. Y.; Luo, K. Q.; Tang, B. Z. Quantitation, Visualization, and Monitoring of Conformational Transitions of Human Serum Albumin by a Tetraphenylethene Derivative with Aggregation-Induced Emission Characteristics. *Anal. Chem.* **2010**, *82*, 7035−7043.
(23) Sharnoff, M. *Photophysics of Aromatic Molecules*; Wiley: London, 2002; Vol. *4*.
(24) Barros, H. L.; Mileski, T.; Dillenburg, C.; Stefani, V. Fluorescent Benzazole Dyes for Bloodstain Detection and Bloody Fingermark Enhancement. *Forensic Chem.* **2017**, *5*, 16−25.
(25) Xu, L.; Li, Y.; Wu, S.; Liu, X.; Su, B. Imaging Latent Fingerprints by Electrochemiluminescence. *Angew. Chem., Int. Ed.* **2012**, *51*, 8068−8072.
(26) Bansal, R.; Sehgal, P.; Bedi, P. Minutiae Extraction from Fingerprint Images - A Review. *Int. J. Comput. Sci. Issues* **2011**, *8*, 74−85.
(27) Wang, M.; Li, M.; Yu, A.; Zhu, Y.; Yang, M.; Mao, C. Fluorescent Nanomaterials for the Development of Latent Fingerprints in Forensic Sciences. *Adv. Funct. Mater.* **2017**, *27*, 1606243.
(28) Chen, H.; Ma, R.-l.; Chen, Y.; Fan, L.-J. Fluorescence Development of Latent Fingerprint with Conjugated Polymer Nanoparticles in Aqueous Colloidal Solution. *ACS Appl. Mater. Interfaces* **2017**, *9*, 4908−4915.
(29) Qiu, Z.; Hao, B.; Gu, X.; Wang, Z.; Xie, N.; Lam, J. W. Y.; Hao, H.; Tang, B. Z. A General Powder Dusting Method for Latent Fingerprint Development Based on AIEgens. *Sci. China: Chem.* **2018**, *61*, 966−970.

DOI: 10.1021/acsami.9b04269
ACS Appl. Mater. Interfaces 2019, 11, 17306−17312